https://doi.org/10.17221/6/2024-JFS

The role of the water regime in a reclaimed limestone quarry

Marcela Burnog, Aleš Kučera*

Department of Geology and Soil Science, Faculty of Forestry and Wood Technology, Mendel University in Brno, Brno, Czech Republic

**Corresponding author: m.burnog@seznam.cz*

Citation: Burnog M., Kučera A. (2024): The role of the water regime in a reclaimed limestone quarry. J. For. Sci., 70: 391–406.

Abstract: This study focused on the hydrophysical characteristics of an abandoned limestone quarry in Czechia. Six sites were examined; two sites were undergoing natural succession (the Quarry Wall and Reed Canary Grass plots, which had undeveloped arboreal layers) and four sites were undergoing managed forest reclamation. Of the four forest reclamation sites, three were classified as prospering (the Prospering Lime, Prospering Maple and Prospering Lime + Oatgrass plots) and one was in decline (the Declining Larch + Lime plot). The arboreal layer included small-leaved lime (*Tilia cordata* Mill.), sycamore maple (*Acer pseudoplatanus* L.), and European larch (*Larix decidua* Mill.). Our results showed that Lime + Oatgrass plot retained more water than other plots. Field soil moisture measurements indicated that throughout the 1096-day monitoring period, only the soils at the successional sites reached the wilting point (Quarry Wall plot: 159 days; Reed Canary Grass plot: 43 days). Soil heterogeneity in the reclaimed areas was due to variation in the soil profile depth, disturbance from mining activities, reclamation efforts, and the availability of quality soil material. Soil conditions and the dynamics at the quarry created less than ideal conditions for tree regeneration. This primarily relates to limiting and significantly heterogeneous successional plots.

Keywords: pedotransfer function; retention curve (RETC) program; soil moisture; tree species

There are now numerous reclamation practices for postmining land restoration, but these practices are not all successful in restoring woody vegetation. Ideally, land restoration should be based on a soil environment assessment that provides information on the environmental limits for different vegetation forms and thus informs potential landscape management (Neri, Sánchez 2010). When forests are used as a means of reclaiming land, managers should create sustainable and ecologically stable forest ecosystems using suitable native or introduced tree species (Vacek et al. 2018; Vacek et al. 2023) and considering soil, original habitat conditions, and the impacts of climate change on forest sustainability (Vacek et al. 2021).

Data on soil suitability provide information on two levels. First, properties such as texture, structure, organic matter content, water holding

Supported by the Internal Foundation Agency of Mendel University, Faculty of Forestry and Wood Technology (IGA LDF_VT_2021006) and by the mining company Českomoravský cement a.s. that enabled the completion of this research.

https://doi.org/10.17221/6/2024-JFS

capacity at different suction pressures, and nutrient content (Ortega et al. 2020; Norouzi et al. 2023; Öztürk et al. 2023) provide basic information about individual soil layers. Second, the total volume of soil, from the surface to the soil-forming substrate, provides data on water storage potential and availability, organic matter storage, and nutrient stocks. This information determines the soil environmental limits in relation to the available nutrient content and available water holding capacity (Ortega et al. 2020; Norouzi et al. 2023).

In early habitat stages, soil depth tends to exceed the rooting zone, meaning that available water sources are rarely limited. This rooting zone deepens as vegetation develops (Leenaars et al. 2018), and the demand for water increases over time to the point where soil depth often becomes a limiting factor in successful forest restoration (Ojekanmi et al. 2020). Hydrologically, the rehabilitation of limestone quarries can be particularly difficult due to their karstic nature (Ganapathi, Phukan 2020). Furthermore, quarry/postmining landscapes are a mosaic of different microhabitats rather than a continuous uniform landscape (Sheoran et al. 2010; Hendrychová et al. 2020). Consequently, soils at postmining quarry sites may lack the necessary properties for forest restoration due to limiting environmental properties, altered soil characteristics, and reduced water availability (Ortega et al. 2020).

Hydrophysical properties, i.e. the link between soil water retention at low suction pressure and soil structure, are an important soil characteristic and are particularly important in the arrangement of soil pores (Hillel 2004; Wang et al. 2023) and in water retention during changes in soil pore spacing caused by frost, compaction, wetting and drying cycles, or the presence of plant roots (Pečan et al. 2023). A soil water retention curve (Öztürk et al. 2023) is commonly used in soil studies (e.g. Javanshir et al. 2020; Fu et al. 2021; Chen et al. 2023; Pham et al. 2023). While such curves have been widely applied in agricultural settings, no study to date has examined soil water retention in a quarry setting.

In this study, soil water retention was assessed in a limestone quarry where previous soil analyses indicated that both trophic and soil hydrophysical properties were limiting factors (Burnog et al. 2022; Burnog et al. 2023). To enhance our understanding of soil water retention mechanisms within areas undergoing restoration, we quantitatively assessed and compared the water storage capacities of prospering and declining forest reclamation sites and successional sites. We hypothesised that the physiological availability of water was the principal factor behind successful vegetation restoration.

MATERIAL AND METHODS

The Mokrá Quarry study site. The Mokrá Quarry (49°13'39.6"N, 16°45'25.1"E) is one of the largest limestone quarries in the Czech Republic and covers an area of 150 ha. It is situated northeast of Brno and borders the Moravian Karst and the Drahanská highlands of southern Moravia. Reclamation work began in the western part of the quarry ca. 30 years ago (Cihlářová et al. 2017). Biogeographically, the quarry falls within the deciduous forests of the Central European province (Cihlářová 2017).

Reclamation efforts have focused on internally stored material (the soil substrate depth is ca. 0.6 m) and have used primarily native tree species, including small-leaved lime (*Tilia cordata* Mill.), pedunculate oak (*Quercus robur* L.), sycamore maple (*Acer pseudoplatanus* L.), Scots pine (*Pinus sylvestris* L.), and European larch (*Larix decidua* Mill.). Despite several successful reforestation efforts, there are areas in the quarry where trees do not thrive. These areas contain dead trees or trees at high risk of mortality. Such trees exhibit slow growth rates and frequently suffer from defects, damage, or dry branches. Additionally, tree trunks may have cavities, cracks, and decaying bark (Burnog et al. 2023).

Six unfenced research plots were delineated within the Mokrá Quarry (Table 1). Two adjacent plots, representing natural succession, the Quarry Wall plot and the Reed Canary Grass plot, were established in the middle of the quarry. The Reed Canary Grass plot represents the floor of a previous level that was last mined ca. 15 years ago. The other four plots represent forest reclamation sites. Three of the forest reclamation plots represent thriving sites (the Prospering Lime, Prospering Maple, and Prospering Lime + Oatgrass plots) and one represents a non-thriving site (the Declining Larch + Lime plot). Forest reclamation initially consisted of the relocation of soil that had been removed prior to limestone extraction, followed by spreading and compaction. Subsequently, tree planting commenced. Reclamation work commenced ca. 25 years ago in the Pros-

https://doi.org/10.17221/6/2024-JFS

Table 1. Description of the study plots

Plot	GPS	Soil surface, relief	Soil depth (cm), stoniness (%)	Vegetation cover	Vegetation vitality
Quarry Wall	49°13'45.36"N, 16°45'55.56"E	scree, slope	10, 70	succession (herbs, shrubs)	sparse, struggling
Reed Canary Grass	49°13'45.42"N, 16°45'55.50"E	shallow loam, flat bottom	15, 35	succession [*Calamagrostis epigejos* (L.) Roth, *Rosa canina* L.]	no symptoms, decrease in vitality
Prospering Lime	49°13'39.72"N, 16°46'21.30"E	loam, gentle slope	80, 10	prospering forest recultivation – underdeveloped herbaceous and shrubby layers, arboreal layer (*Tilia cordata* Mill.)	vital tree
Prospering Maple	49°13'39.18"N, 16°46'10.26"E	loam, gentle slope	80, 10	prospering forest recultivation – underdeveloped herbaceous and shrubby layers, arboreal layer (*Acer pseudoplatanus* L.)	vital tree
Declining Larch + Lime	49°13'38.04"N, 16°46'18.60"E	loam, plain	40, 30	declining forest recultivation – herbaceous layer [*Arrhenatherum elatius* (L.) Beauv. ex J. et C. Presl] dominant, arboreal layer (*Larix decidua* Mill., *Tilia cordata* Mill.)	dead trees (lime, larch), low growth rate (lime), defective or damaged branches and dry branches (lime), trunks have cavities (lime, larch), cracks and occasionally rotten bark (lime)
Prospering Lime + Oatgrass	49°13'38.58"N, 16°46'19.14"E	loam, plain	65, 10	prospering forest recultivation – vital herbaceous tree layer [*Arrhenatherum elatius* (L.) Beauv. ex J. et C. Presl] dominant, arboreal layer (*Tilia cordata* Mill.)	vital tree

pering Lime and Prospering Maple and ca. 20 years ago in the Declining Larch + Lime and Prospering Lime + Oatgrass plots.

To date, there has been no systematic inventory of the forest plantations and no silvicultural intervention (Sekanina, Musilová 2011; Cihlářová 2017). The frequency of planting of individuals of each tree species (one thousand per ha) corresponded to applicable legislation (Decree No. 456/2021 Coll., issued by the Ministry of Agriculture of the Czech Republic on November 29, 2021) and the plantations were supplemented during the seven years after planting.

Natural conditions. The Mokrá Quarry is composed of rocks from the Middle and Upper Devonian periods, and the substrate consists of Devonian clastics deposited on the Brno igneous massif. In addition to limestone, culm and slate are found in the eastern part of the quarry (Sekanina, Musilová 2011; Zimák et al. 2018). The study area lies at 350 m a.s.l. to 440 m a.s.l. (Burnog et al. 2023) and falls within two watersheds: the Hostěnický stream watershed merges into the Říčka river via the Hostěnický sinkhole, and the Mokerský (Vlašnovský) stream watershed merges with the Rokytnice stream on its right bank and later com-

https://doi.org/10.17221/6/2024-JFS

bines with the Říčka river downstream (Sekanina, Musilová 2011). The site is classified as moderately warm (regional classification MT – 10) according to the system of Quitt (1971). July air temperatures range from 16 °C to 18 °C and January air temperatures range from –2 °C to –5 °C. Annual precipitation in the region fluctuates between 550 mm and 750 mm. Temperature and precipitation measurements carried out at the Mokrá Quarry between 2013 and 2014 indicated an average annual temperature of 9.4 °C and annual precipitation of 461.7 mm (Cihlářová et al. 2017).

The soils around the quarry contain a considerable amount of limestone gravel, which enriches the soil with calcium and increases the local pH. In terms of water supply, the soil body is generally shallow and may be water-deficient (Mackovčin et al. 2007). Limestone bedrock is commonly covered with loess material and forms geoabruptic Alfisols (Episiltic, Cutanic, and Epidystric) according to Soil Survey Staff 2014, with two different clay origins in the main soil strata: clay from illimerisation processes and clay of *terra fusca* paleosol origin, which is unchanged and conserved by the limestone. While the mine was operational, different quantities of different layers (0.5–1.0 m) were extracted and later redeposited after closure of the quarry as a 0.4–0.7 m anthropogenic substrate.

Within the study plots (see below), soils are classified as Spolic Leptic Technosols (Loamic, Amphidensic, Hypereutric, Protic, Raptic, Relocatic, and Terric), according to Soil Survey Staff 2014, and are often in shallow lithological contact with limestone and could play a substantial role in postmining forest restoration. Soil analysis in previously reclaimed areas revealed deficiencies in nitrogen, phosphorous, and carbon and excess calcium and magnesium. Soil pH was neutral, usually reaching values greater than 6.5 (pH/KCl; Burnog et al. 2022). The soil organic carbon content was 1.86%, and the total nitrogen content was 0.17%. The resulting carbon : nitrogen ratio fell within the favourable range of 8–18. The predominant soil texture was silty-clay loam, with relatively uniform soil properties with depth and an admixture of artefacts, rubble and scoria due to the mixed anthropogenic origin of the substrate.

Data collection and field work. A VIRRIB LP soil moisture sensor (AMET Co., Czech Republic) was installed in each plot in the summer of 2019. All sensors were installed at 15 cm depth, except in the Quarry Wall plot, where soils were closer to 10 cm depth. Starting in October 2019, data were collected at one-hour intervals and stored on a MeteoUNI data logger (AMET Co., Czech Republic). Daily mean values over a hydrologic year from 1 November to 31 October (Scott et al. 2015) were calculated. Volumetric moisture Θ (%) measurements continued until October 2022, thereby providing a long-term soil moisture dataset over three hydrological years (2020–2022). Soil moisture data were compared with daily precipitation totals from the nearest meteorological station (Brno-Tuřany, 49°9'10.8'N, 16°41'19.68''E) and the Czech Hydrometeorological Institute (Brno Branch). On April 5, 2023, homogeneous undisturbed soil samples were collected from each site using a metal sampling cylinder (Kopecký's 100 cm^3 physical volumeter), with three samples taken at the vertices of a triangle at a depth equivalent to the moisture sensor installations (i.e. 10–18 cm). These samples were hermetically sealed and transported to the laboratory for analysis.

Soil analysis. All soil samples underwent analysis in their undisturbed state, following the procedure of Hillel (2004). Briefly, samples were weighed at four water status stages: (*i*) after full water saturation m_s; (*ii*) after 24 h desuction on three filter papers (under a cover eliminating water evaporation from the sample surface), thus expressing field capacity m_{33}; (*iii*) after air-drying at 60% air humidity, thus expressing normal hygroscopicity Vh_n; and (*iv*) after oven-drying at 105 °C until a constant weight m_d was achieved. Soil particle density ρ_s was determined using the pycnometric method (g·cm^{-3}), and bulk density r_d (g·cm^{-3}), porosity P (%), moisture content Θ (%), full water saturation capacity Θ_s (%), field water saturation capacity Θ_{33} (%), normal hygroscopicity Vh_n (%), and residual water saturation capacity Θ_r (%) were measured. The soil exchangeable reaction (pH/KCl) was assessed in 0.2 M KCl solution with a soil : eluent ratio of 1 : 2.5 using a pH meter with a combined electrode. Particle size distribution was determined using the sedimentation-pipette method for particles with a diameter < 0.05 mm and by wet sieving for particles with a diameter > 0.05 mm (Soil Survey Staff 2014), based on basic grain size fractions of < 0.002 mm, 0.002–0.05 mm, and 0.05–2 mm, following the soil type classification standards according to the United States Department of Agriculture, Natural Resources

https://doi.org/10.17221/6/2024-JFS

Conservation Service (USDA-NRCS). Total organic carbon was determined using the combustion method (DIN 19539 2016). Briefly, 200 mg ± 15 mg samples were ground in an MM 400 oscillating mill (Retsch GmbH, Germany) and then dried in a UF 260 Universal Oven (Memmert GmbH, Germany) for 24 h at 80 °C. The samples were then measured on a SoliTOC analyser (Elementar Analysensysteme GmbH, Germany) using temperature-dependent differentiation of total carbon and total inorganic carbon burned at 900 °C. The temperature was gradually increased from 400 °C to 600 °C and then to 900 °C at a constant heating rate of 70 $K \cdot min^{-1}$ using an oxygenated atmosphere and a nitrogen carrier.

Data processing. Water retention curves were produced using pedotransfer functions (*pF*s) derived from the ROSETTA module of the RETC program (Version 6.02, 2009; Van Genuchten et al. 1991), using the hydraulic parameters of van Genuchten (1980) as inputs for the retention model. The model expresses the volumetric moisture content ($cm^3 \cdot cm^{-3}$) as Equation (1):

$$\Theta(h) = \Theta_r + \frac{\Theta_s - \Theta_r}{\left[1 + \left(\alpha h\right)^n\right]^{\frac{1-1}{n}}} \quad (1)$$

where:

$\Theta(h)$ – observed volumetric moisture content ($cm^3 \cdot cm^{-3}$);

h – soil matrix suction (cm in positive increasing values);

Θ_r – residual moisture content ($cm^3 \cdot cm^{-3}$);

Θ_s – saturated moisture content ($cm^3 \cdot cm^{-3}$);

α, n, m – empirical coefficients indicating the shape or curvature of the retention curve, where $\alpha > 0$ (cm^{-1}), $n > 1$, and $m = 1 - \frac{1}{n}$.

When assessing the optimal *pF* algorithm, hydraulic function parameters were predicted using the equations of van Genuchten (1980) and the Maulem module integrated into the ROSETTA module of the RETC program, allowing inclusion of the percentage of sand, silt, and clay (r_d, Θ_s, and Θ_{33}).

The *pF* retention curves, which describe the relationship between volumetric water content and suction pressure, were then used to determine the following hydrolimits: maximum capillary capacity Θ_{MCC} at *pF* 1.6–2.0, water retention capacity Θ_{WRC} at *pF* 2.0–2.7, and wilting point Θ_{WP} at *pF* 4.18. The available water capacity *AWC* (mm of water column in 100 mm of soil mass column) was calculated as the difference between Θ_{WRC} and Θ_{WP}. The plant available water supply *PAWS* [mm·(100 mm)$^{-1}$] was calculated as the difference between Θ and Θ_{WP}. A binary scoring system (0/1) was then used to quantify water status, with daily mean soil moisture values > Θ_{MCC} and Θ_{WRC} and < Θ_{WP} scored as 1 and soil moisture values < Θ_{MCC} and Θ_{WRC} and > Θ_{WP} scored as 0.

RESULTS

Soil conditions. The soil bulk density in all plots ranged from 1.54 $g \cdot cm^{-3}$ to 1.92 $g \cdot cm^{-3}$ and peaked in the Quarry Wall plot (Table 2).

Soils in the successional plots and the Declining Larch + Lime plot exhibited greater stoniness, with values ranging from 30% to 70%, than soils from the other sites (10%; see Table 1). Porosity varied between plots, ranging from 23.68% to 38.04% (Table 2), with the highest porosity recorded in the flat-bottomed succession site where the clay content was high. The soil texture was classified as silty-clay-loam in the forest reclamation

Table 2. Soil bulk density (r_d), porosity (*P*), moisture (Θ), soil reaction (pH/KCl), clay content, silt content, sand content, total organic carbon (*TOC*), and total inorganic carbon at 900 °C (*TIC*900) in each of the study plots

Plot	r_d ($g \cdot cm^{-3}$)	*P* (%)	Θ (%)	pH/KCl	Clay (%)	Silt (%)	Sand (%)	Texture	*TOC* (%)	*TIC*900 (%)
Quarry Wall	1.92	26.82	35.18	7.27	27.73	40.07	32.20	loam/clay loam	0.64	4.92
Reed Canary Grass	1.54	38.04	44.21	7.20	42.63	54.17	3.20	silty clay	1.36	5.57
Prospering Lime	1.55	23.68	36.54	4.77	31.07	64.30	4.63	silty clay loam	0.63	0.04
Prospering Maple	1.59	26.97	37.30	6.27	37.53	55.47	7.00	silty clay loam	0.60	0.04
Declining Larch + Lime	1.74	24.56	38.90	6.97	31.90	59.97	8.13	silty clay loam	0.52	0.92
Prospering Lime + Oatgrass	1.59	36.23	36.79	6.80	36.67	55.43	7.90	silty clay loam	0.58	0.75

https://doi.org/10.17221/6/2024-JFS

sites and silty-to-loamy clay and clay-loam in the succession sites. Soils in the successional plots had higher potential soil reaction (neutral to slightly alkaline) than those in forest reclamation plots. Most sites had similar soil reactions, except for the Prospering Lime plot, which had the lowest value of 4.77. The Reed Canary Grass successional site had the highest total organic carbon content, at 1.36%, and the forest reclamation plots had much lower values.

Soil water retention curves and available water. At all the sites, the saturated moisture content (*pF* 0) ranged from 47.7% to 42.0%, with maximum values recorded in the Reed Canary Grass plot (Figure 1). Differences were observed between the succession sites; soil samples that contained the highest concentration of clay particles (from the Reed Canary Grass plot) exhibited the greatest changes in moisture and the highest soil water retention (Table 3). A noticeable reduction in volumetric moisture content occurred in all samples at suction pressures of *pF* 1.5 or higher, with a considerable reduction in the highest saturated Reed Canary Grass sample. Wilting points varied from 15.1% to 11.0% across all sites, with reclaimed forest sites showing the greatest difference (11.0% to 13.7%) and the successional sites remaining relatively unchanged (Table 3). It should be noted, however, that wilting points at the successional sites were reached at higher moisture levels than wilting points at the reclaimed forest sites.

For the reference 10 cm of soil, water availability was uniform. For the entire soil profile, values differed markedly; the lowest values occurred in the Quarry Wall and Reed Canary Grass plots, followed by the Declining Larch + Lime plot.

Soil moisture dynamics. Noticeable fluctuations in soil moisture content occurred over the 1 096 days of measurement (Figures 2–7). Forest reclamation sites had higher average soil moisture (during the years 2020–2022) than did successional sites (Table 4). The highest average moisture value

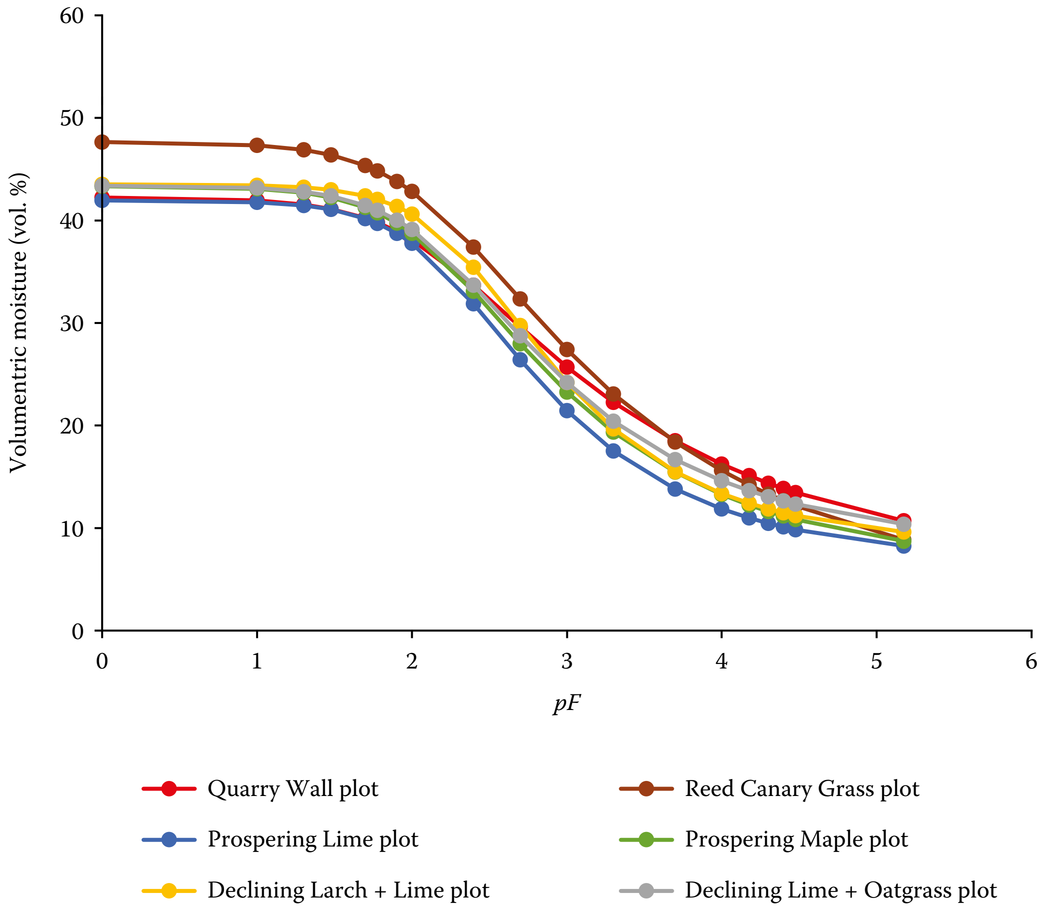

Figure 1. Soil retention curves for the plots

pF – pedotransfer function

https://doi.org/10.17221/6/2024-JFS

Table 3. Wilting point (Θ_{WP}), water retention capacity (Θ_{WRC}), maximum capillary capacity (Θ_{MCC}) and available water capacity (*AWC*) at the reclamation areas

Plot	Θ_{WP} (vol. %)	Θ_{WRC} (vol. %)	Θ_{MCC} (vol. %)	*AWC* [mm·(10 cm)$^{-1}$]	*AWC* [mm·(soil profile)$^{-1}$; Table 1]
Quarry Wall	15.1	32.1	40.2	17.0	17.0
Reed Canary Grass	14.2	35.4	45.3	21.2	31.8
Prospering Lime	11.0	29.7	40.2	18.7	149.6
Prospering Maple	12.2	31.1	41.3	18.8	150.4
Declining Larch + Lime	12.4	33.3	42.4	20.8	83.3
Prospering Lime + Oatgrass	13.7	31.7	41.5	18.1	117.4

was recorded in the Prospering Lime + Oatgrass plot (41.28%). Conversely, the lowest average moisture (23.32%) was recorded in the Quarry Wall plot. Minimum soil moisture content in the reclaimed plots ranged from 6.20% in the Quarry Wall plot to 22.51% in the Prospering Lime + Oatgrass plot, maximum soil moisture in the Prospering Maple plot (60.01%) and in the Prospering Lime plot (56.94%), and all other reclaimed areas exhibited values of approximately 49%.

Hydrological limits were reached during measurement (Table 5; Figures 2–7). The Prospering Lime + Oatgrass plot experienced 386 days that surpassed the maximum capillary capacity (Figure 7), while the Quarry Wall plot had the lowest count, at only 34 days (Figure 2). The Prospering Lime + Oatgrass plot experienced 1 020 days above the soil water retention capacity (Figure 7). The wilting point was only reached at natural succession sites (Figures 2–3). Soil moisture in the Quarry Wall plot dropped below the wilting point on 159 days (Figure 2), with 154 of those days occurring during the growth season, and the Reed Canary Grass plot dropped below the wilting point on 43 days

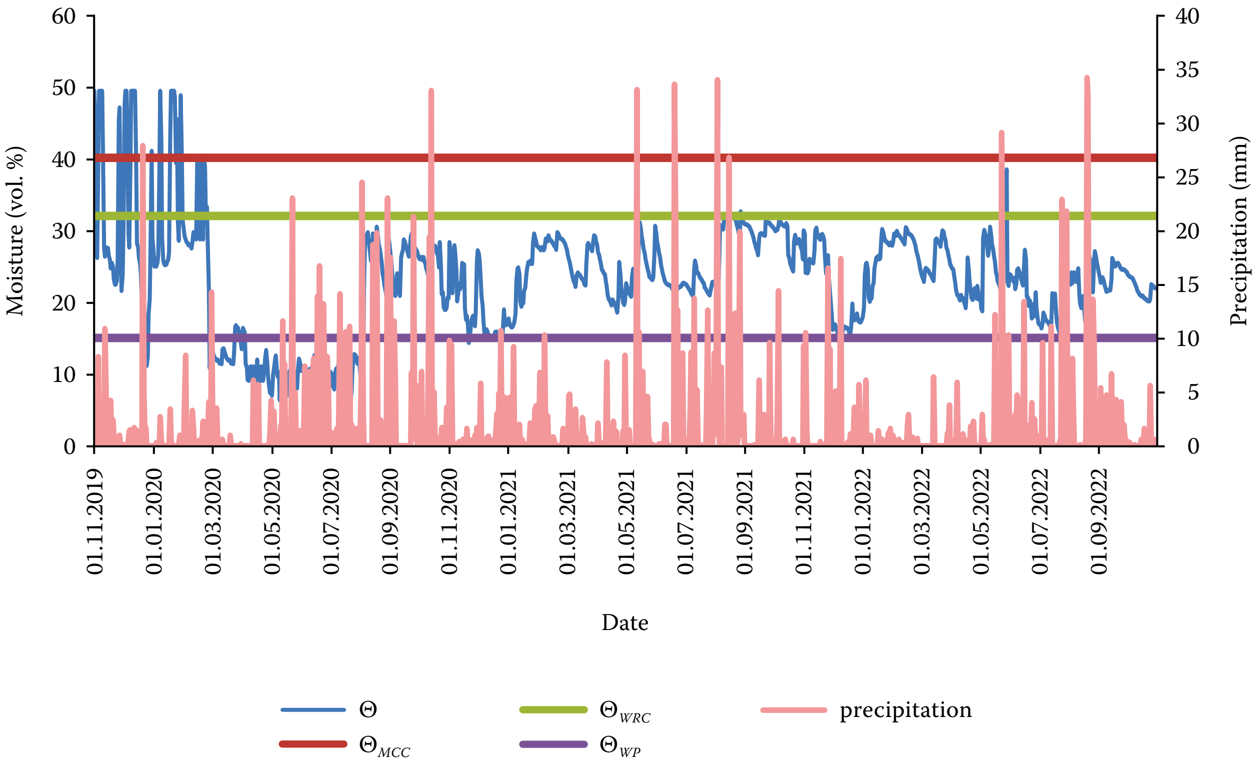

Figure 2. Soil moisture and daily precipitation at the Quarry Wall plot

Θ – soil volumetric moisture; Θ_{MCC} – maximum capillary capacity; Θ_{WRC} – water retention capacity; Θ_{WP} – wilting point

https://doi.org/10.17221/6/2024-JFS

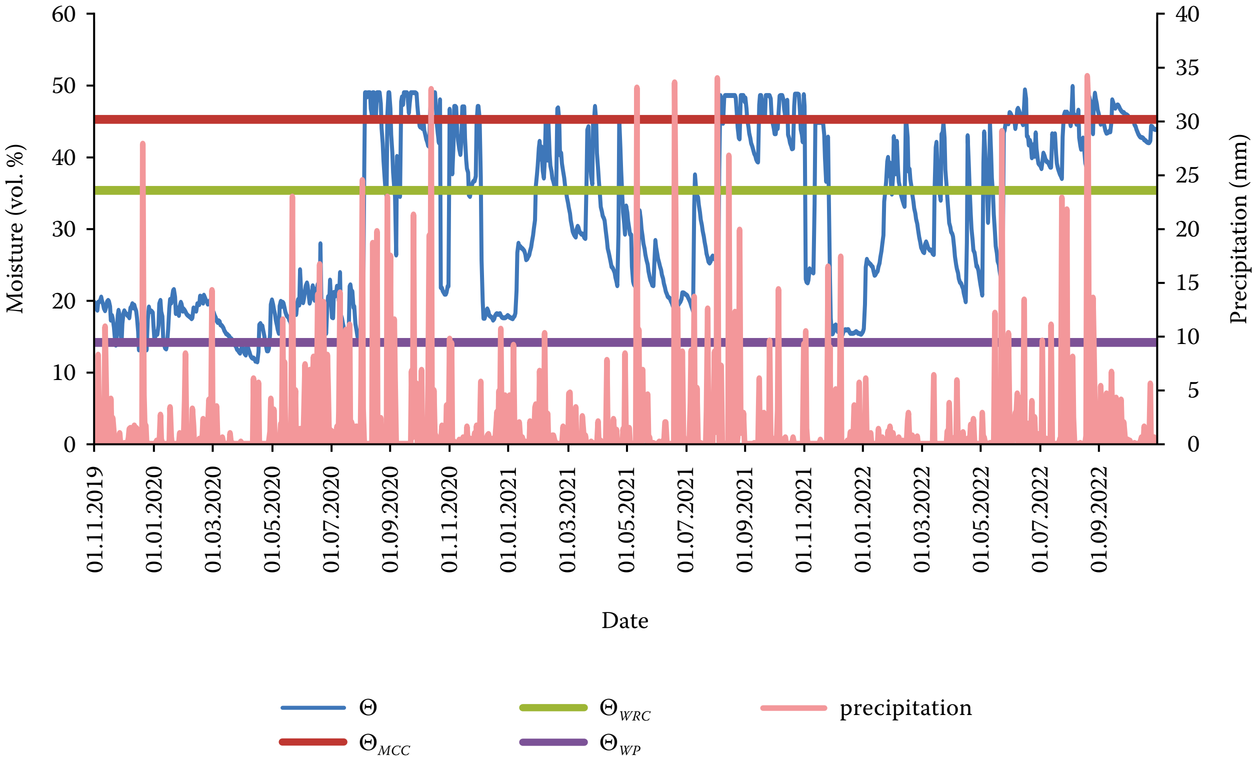

Figure 3. Soil moisture and daily precipitation at the Reed Canary Grass plot

Θ – soil volumetric moisture; $Θ_{MCC}$ – maximum capillary capacity; $Θ_{WRC}$ – water retention capacity; $Θ_{WP}$ – wilting point

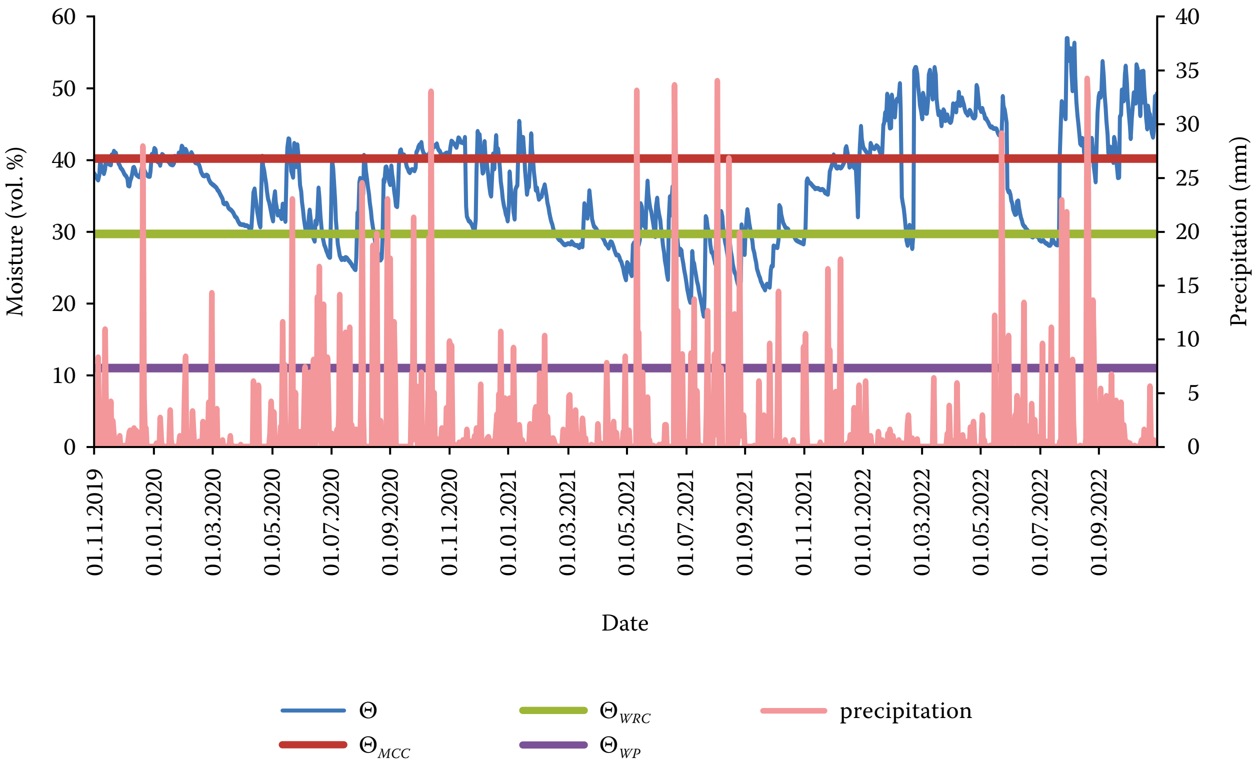

Figure 4. Soil moisture and daily precipitation at the Prospering Lime plot

Θ – soil volumetric moisture; $Θ_{MCC}$ – maximum capillary capacity; $Θ_{WRC}$ – water retention capacity; $Θ_{WP}$ – wilting point

https://doi.org/10.17221/6/2024-JFS

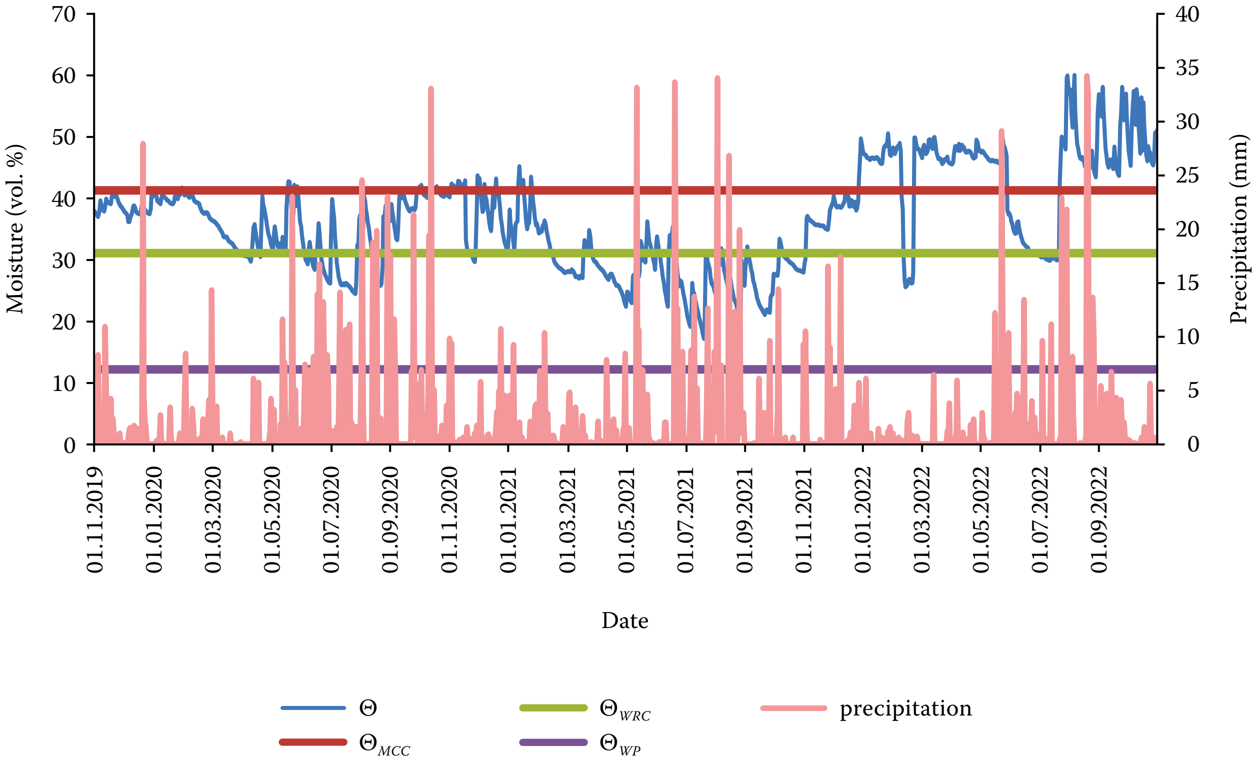

Figure 5. Soil moisture and daily precipitation at the Prospering Maple plot

Θ – soil volumetric moisture; $Θ_{MCC}$ – maximum capillary capacity; $Θ_{WRC}$ – water retention capacity; $Θ_{WP}$ – wilting point

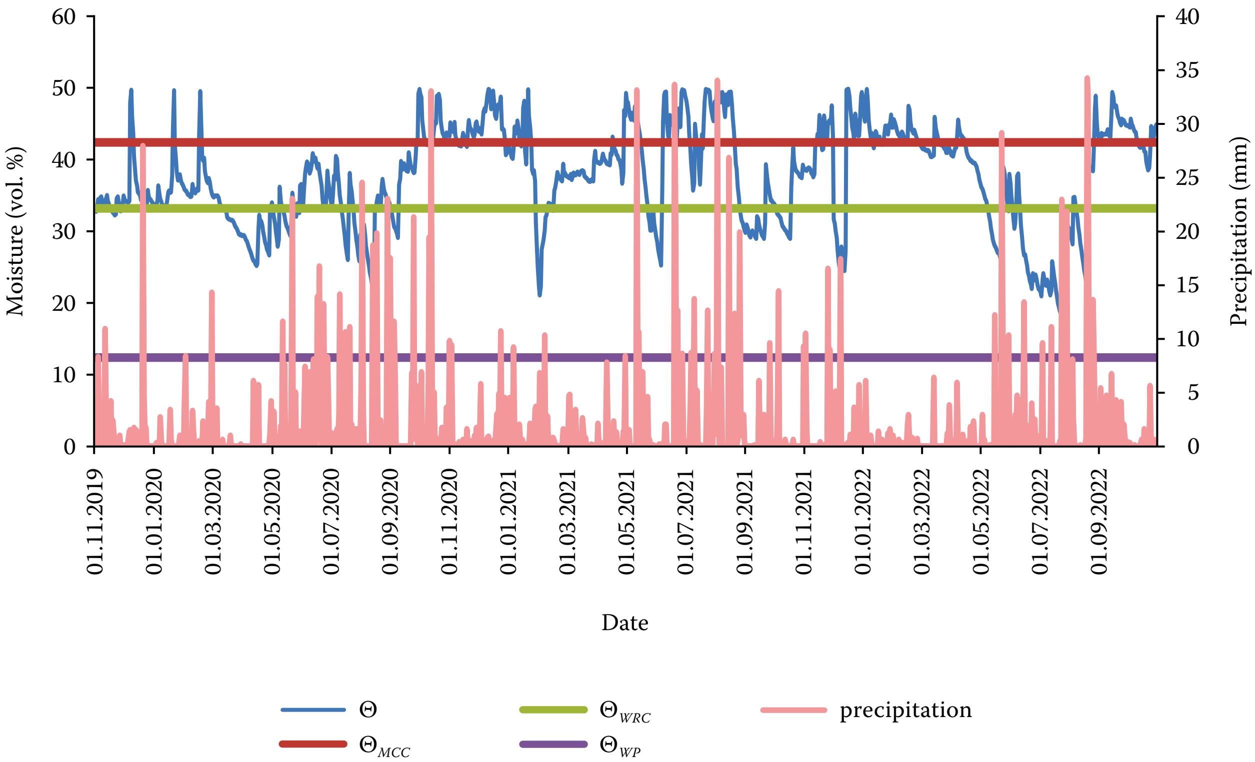

Figure 6. Soil moisture and daily precipitation at the Declining Larch + Lime plot

Θ – soil volumetric moisture; $Θ_{MCC}$ – maximum capillary capacity; $Θ_{WRC}$ – water retention capacity; $Θ_{WP}$ – wilting point

https://doi.org/10.17221/6/2024-JFS

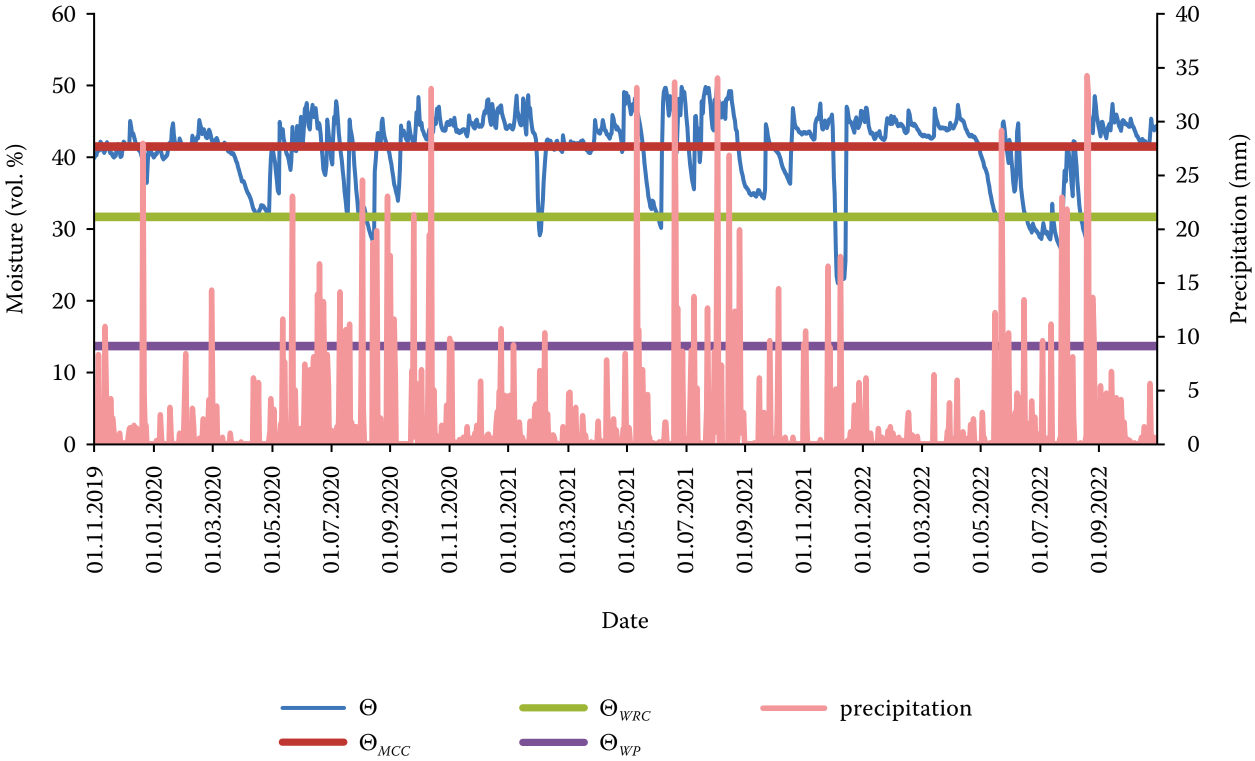

Figure 7. Soil moisture and daily precipitation at the Prospering Lime + Oatgrass plot

Θ – soil volumetric moisture; Θ_{MCC} – maximum capillary capacity; Θ_{WRC} – water retention capacity; Θ_{WP} – wilting point

(Figure 3), with 33 of those days occurring during the growth season. During this study, the *AWC* interval between Θ_{WP} and Θ_{WRC} remained relatively constrained for 889 days in the Quarry Wall plot. Conversely, the Prospering Lime + Oatgrass plot reached this interval for 76 out of 1 096 days of measurement (Table 5; Figures 2–8).

The successional plots were limited in *PAWS* for some periods during the study (Figure 8). In particular, the Quarry Wall plot reached values below 0, indicating a substantial lack of water during the 2020 growing season. In the following years, the soil water status was similar in both successional plots and reached the wilting point for at least 3 consecutive weeks.

The moisture status also differed with respect to plant available water dynamics, as indicated by the coefficient of variation. The values of the coefficient of variation of *PAWS* suggested more diverse and variable water resources in the successional sites than in the forest reclamation sites (Table 6). The successional plots exhibited more extreme conditions that limited the development of woody vegetation.

Table 4. Average soil moisture (*ASM*; vol. %) in the plots over three consecutive hydrological years (2020–2022)

Plot	*ASM* 2020	*ASM* 2021	*ASM* 2022	*ASM* 2020–2022	Min. soil moisture 2020–2022	Max. soil moisture 2020–2022
Quarry Wall	21.79	24.78	23.40	23.32	6.20	49.50
Reed Canary Grass	23.65	33.45	35.54	30.88	11.49	49.90
Prospering Lime	36.13	30.90	41.95	36.33	18.22	56.94
Prospering Maple	35.91	30.27	43.59	36.59	17.22	60.01
Declining Larch + Lime	34.99	39.92	38.00	37.64	18.06	49.80
Prospering Lime + Oatgrass	40.59	42.76	40.50	41.28	22.51	49.78

https://doi.org/10.17221/6/2024-JFS

Table 5. Occurrences of hydrolimits during the measurement of soil moisture, including the number of days above the maximum capillary capacity (Θ_{MCC}) and water retention capacity (Θ_{WRC}), below the wilting point (Θ_{WP}), and the available water capacity (*AWC*) within the *WP*–*WRC* interval

Plot	Θ_{MCC}	Θ_{WRC}	Θ_{WP}	*AWC*
Quarry Wall total	34	48	159	889
2020	34	45	154	167
2020 March–October	0	0	148	97
2021	0	2	4	359
2021 March–October	0	2	0	243
2022	0	1	1	363
2022 March–October	0	1	1	243
Reed Canary Grass total	179	459	43	594
2020	48	75	43	248
2020 March–October	48	75	33	137
2021	70	166	0	199
2021 March–October	58	106	0	139
2022	61	218	0	147
2022 March–October	59	180	0	65
Prospering Lime total	359	839	0	257
2020	85	322	0	44
2020 March–October	49	201	0	44
2021	38	188	0	177
2021 March–October	0	79	0	166
2022	236	329	0	36
2022 March–October	182	215	0	30
Prospering Maple total	292	765	0	331
2020	20	299	0	67
2020 March–October	16	178	0	67
2021	29	137	0	228
2021 March–October	0	36	0	209
2022	243	329	0	36
2022 March–October	191	223	0	22
Declining Larch + Lime total	333	805	0	291
2020	37	243	0	123
2020 March–October	16	135	0	110
2021	149	296	0	69
2021 March–October	83	189	0	56
2022	147	226	0	99
2022 March–October	64	159	0	86
Prospering Lime + Oatgrass total	386	1 020	0	76
2020	44	353	0	13
2020 March–October	34	232	0	13
2021	163	358	0	7
2021 March–October	87	241	0	4
2022	179	309	0	56
2022 March–October	86	200	0	45

https://doi.org/10.17221/6/2024-JFS

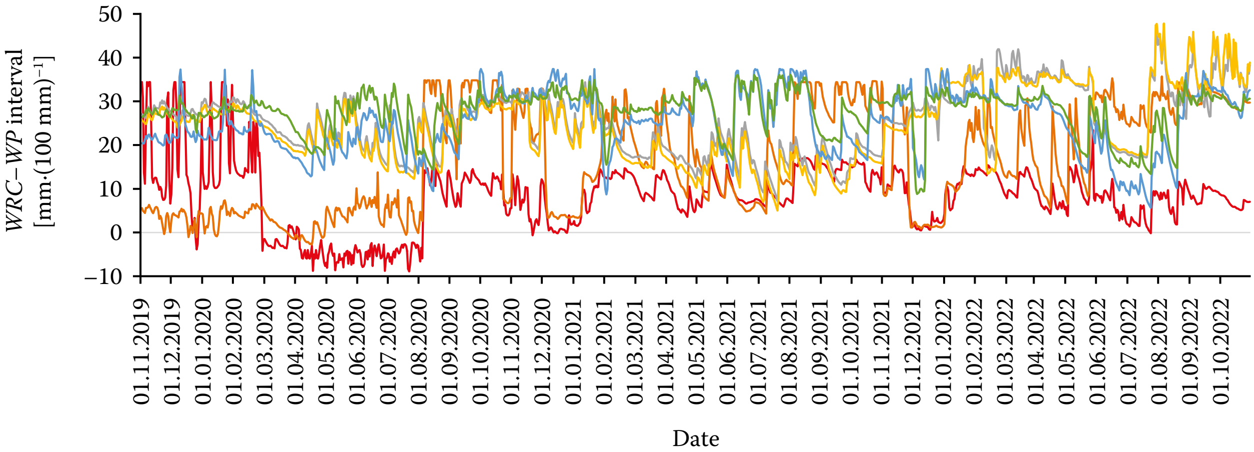

Figure 8. Plant available water supply (*PAWS*) in the plots

WRC–WP – interval between water retention capacity and wilting point

Table 6. Coefficient of variation of instantaneous usable water in the plots

Plot	Coefficient of variation
Quarry Wall	0.94
Reed Canary Grass	0.72
Prospering Lime	0.29
Prospering Maple	0.34
Declining Larch + Lime	0.28
Prospering Lime + Oatgrass	0.18

DISCUSSION

Soil properties. As noted by Buondonno et al. (2018), soil quality is a key factor in achieving effective quarry restoration. Soil substrates in postmining limestone quarries tend to be poor and are generally classified as Technosols (Nanko et al. 2014; IUSS Working Group WRB 2022; Burnog et al. 2023). Owing to the extreme conditions found in quarries, natural recovery can be very slow (Luna et al. 2016; Carabassa et al. 2020); hence, the reclamation of limestone quarries usually begins with laying an insert substrate that consists of easily fragmented material, partly to prevent erosion from typically steep slopes but also to provide a growing surface for vegetation (Cihlářová 2017; Pečan et al. 2023). In this study, we focused on the impact of the heterogeneity of soil properties in the limestone quarry. We found that soil in the Quarry Wall plot had the highest bulk density (1.92 g·m^{-3}) among the plots. This factor, in combination with porosity (26.82%) and texture (loam/clay loam), may limit the water regime, air exchange, and root growth (Nanko et al. 2014; Cui et al. 2019). Due to a higher sand content (Table 2) and the slope of the terrain, this site may be more susceptible to rapid runoff and soil erosion (Liu et al. 2019).

Soils from areas of natural succession were slightly alkaline due to the presence of limestone quarrying waste, which had a distinct effect on local vegetative cover and soil reactions (Table 1; see also Bellmann et al. 2016; Šikula, Větvička 2016; Štursa 2016; Kaplan et al. 2019). Soils from the forest reclamation sites (the Prospering Lime and Prospering Maple plots) were slightly acidic, which is conducive to many tree species (Bellmann et al. 2016; Kaplan et al. 2019), including the predominant species at the sites (Table 1). Interestingly, the one site with poor tree growth, the Declining Larch + Lime plot, had soil with a neutral pH. Neither lime nor larch, which tolerates a wide range of soil conditions, thrived at the site. This site had the highest soil reaction values of any of the forest reclamation sites, which may be one of the reasons for the less successful growth of lime. Furthermore, the Declining Larch + Lime plot had a total

https://doi.org/10.17221/6/2024-JFS

soil depth of only 40 cm; this is also likely to have contributed to tree decline because both lime and larch prefer deeper soils. Since the other forest reclamation sites had deeper soil profiles, we can conclude that a depth of ca. 40 cm was limiting for tree growth at this site. This condition was also noted by Welegedara et al. (2020), who observed improved growth in deeper soils when planting trees at depths of 35 cm, 50 cm, and 100 cm.

Soil water availability. Increased drought and water scarcity are major threats of climate change (Ahmad et al. 2022; Zeng et al. 2023). In this context, Vacek et al. (2021) proposed afforesting after logging with adaptable tree species. Research has shown that *Pinus sylvestris*, *Pinus nigra*, *Larix decidua*, *Pseudotsuga menziesii*, and *Picea omorika* are among the most resilient tree species in response to climate extremes. The highest biomass, wood production, and carbon stocks were recorded in *Pinus nigra*, *Pseudotsuga menziesii*, and *Pinus sylvestris*. Introduced conifers (*Pinus nigra* and *Pseudotsuga menziesii*) have been shown to lead to greater carbon accumulation in forest floor humus than deciduous trees; however, introduced species may also lead to a decrease in biodiversity at the stand level and introduce pests and pathogens into the forest ecosystem (Vacek et al. 2021; Vacek et al. 2023).

The low sand/high clay soils in our study exhibited reduced water drainage, greater wilting point and lower water plant availability, and limited soil aeration during wet periods, which was linked with a lack of microporosity. The Reed Canary Grass and Quarry Wall plots exhibited shallow soil profiles devoid of forest layers. Soil moisture measurements frequently reached the wilting point in these plots, with the Quarry Wall plot experiencing the most days when water was unavailable to plants. The extremely shallow root systems of plants in the Reed Canary Grass plot caused brief periods of soil water retention and short-term attainment of the wilting point (Ferrate et al. 2014; Qiu et al. 2023); these transient soil drying conditions were found to be optimal for wood small-reed (Šikula, Větvička 2016). Table 5 and Figure 8 demonstrate that the instantaneous usable water stocks in the Prospering Lime + Oatgrass, Prospering Lime, Prospering Maple, and Declining Larch + Lime plots appeared to be adequate. According to Garcia et al. (2018), global forested areas currently maintain sufficient water reserves. However, concerns about future water consumption in forests are growing, especially in regions already facing limited water availability. This issue may also arise in quarry areas where extreme climatic conditions prevail (Burnog et al. 2023). As the arboreal layer in a quarry becomes older, the water demand could exceed the supply (Garcia et al. 2018). In the Mokrá Quarry, the Quarry Wall and Reed Canary Grass plots were unable to adequately supply water to the vegetation due to pedological, moisture-related, and spatial characteristics (Tables 1, 2, and 5). Together, the *PAWS* (Figure 8) and the shallower soil depth in the Declining Larch + Lime plot, created stressful conditions for trees during the growing season. The year 2022 had a confirmed water deficiency, which was similar to conditions observed in the Quarry Wall plot from 2019 to 2022. Clearly, soil depth and stoniness limit the total available soil water capacity and predispose habitats to drought stress.

Water retention curves displayed a dynamic relationship between plots, with the most notable differences in water content between reclamation sites occurring primarily at higher matrix potentials. The amount of water retained at matrix potentials between 0 bar and 1 bar, which reflects the shape of the water retention curve, depends mainly on the soil capillary effect and pore size distribution (Hillel 2004). As expected, the steepness of the retention curves indicated that the successional Reed Canary Grass plot and the Declining Larch + Lime forest reclamation plot lost water more rapidly than the other sites, a situation that can lead to plant dehydration and subsequent dieback (Walters et al. 2023).

Soil moisture and precipitation dynamics. Differences in the coefficients of instantaneous usable water stocks (Table 6) highlight intriguing disparities in hydrological dynamics. Factors contributing to this variability include soil depth and vegetation cover (Lin et al. 2022; Pečan et al. 2023). Shallower soils with limited vegetation cover may rapidly respond to precipitation events, particularly soils with a higher sand content (e.g. the Quarry Wall plot). Moreover, a lower coefficient of variation in forest reclamation sites potentially has important implications for ecosystem stability and water resource management.

In 2022, the average annual precipitation for this region was the lowest (514.1 mm) recorded during the observation period (2020: 574.7 mm;

https://doi.org/10.17221/6/2024-JFS

2021: 621 mm, according to data from the Czech Hydrometeorological Institute); however, the average soil moisture content for the same year was the highest over the same period (Figures 2–7). According to Pečan et al. (2023), areas with more trees and herbaceous cover influence the structural dynamics of the soil and the subsequent shape of the soil water retention curve. In our case, areas without arboreal cover did indeed exhibit lower average soil retention; the Quarry Wall plot, which lacked any developed forest canopy, had reduced water retention capacity compared with the Reed Canary Grass plot, where herbaceous and light shrub layers were well developed. During growth, tree roots tend to compress the soil, creating channels that can accelerate the horizontal and vertical movement of water and increase the rate of soil water infiltration. Shrub and grass roots are shallow and do not form root channels as effectively as tree roots (Qiu et al. 2023). Consequently, grass root systems only have access to water at or near the surface (Ferrante et al. 2014), suggesting that the shallow root systems typical of successional areas may have had an increased ability to absorb water, although they may not have been able to retain water over the long term. Our results indicate that the forest reclamation sites were better able to retain water in the soil over time. Furthermore, since soils at successional sites are considerably shallower (0.10–0.15 m) than those at forest reclamation sites (0.40–0.80 m), plant water availability plays a crucial role in the reference depth for soil sensor installation and in the entire soil body (Prescott et al. 2019).

CONCLUSION

Considerable soil heterogeneity occurred among the reclaimed areas. Soil profile depth, soil structure, and vegetation cover influenced the hydrophysical properties in the Mokrá Quarry. Soil moisture analysis revealed that the Prospering Lime + Oatgrass plot retained the most water (Θ_{MCC}: 386 days; Θ_{WRC}: 1 020 days; Θ_{WP}: 0 days; and *WRC*–*WP* interval: 76 days) over the 1 096-day monitoring period. Overall, soils with a profile deeper than 65 cm retained more water. Shallow soils without an arboreal layer reached the wilting point more often (Quarry Wall plot: 159 days; Reed Canary Grass plot: 43 days). Based on the retention curves, the Reed Canary Grass plot lost the most water over time. Our study highlights the crucial role of soil quality and depth in determining the success of reclamation efforts. It is evident that the heterogeneity of current soil conditions and the dynamics of natural conditions at the Mokrá Quarry still do not create ideal conditions for tree regeneration. Based on the limiting and heterogeneous successional plots with decreased water retention, we suggest that water availability for plants should be improved through the addition of organic matter to the soil.

In the future, the differences between successional and reclaimed sites and the effect of vegetation type on soil water flow should be investigated. In particular, dendrological surveys would be valuable, given the limited data on this vegetation type. The planting of appropriate trees (both indigenous and non-native species) may restore forest reclamation areas that are in decline and increase biodiversity. In such cases, native species (e.g. *Quercus robur* and *Tillia cordata*) can aid in restoring original ecological interactions and supporting local biodiversity, while introduced species (e.g. *Pinus nigra* and *Pseudotsuga menziesii)* can introduce new adaptive capabilities and potentially increase forest resilience to climate change.

Acknowledgement: The authors would like to thank Dr. Kevin Roche for proofreading and native English language correction.

REFERENCES

Ahmad M.M., Yaseen M., Saqib S.E. (2022): Climate change impacts of drought on the livelihood of dryland smallholders: Implications of adaptation challenges. International Journal of Disaster Risk Reduction, 80: 1–11.

Bellmann H., Wolfgang H., Spohn M., Steffen S. (2016): Poznáváme rostliny: Přes 900 druhů rostlin, mechorostů a hub. Prague, Knižní klub: 447. (in Czech)

Buondonno A., Capra G.F., Di Palma D., Grilli E., Vigliotti R.C. (2018): Pedotechnologies for the Environmental Reclamation of limestone quarries. A protocol proposal. Land Use Policy, 71: 230–244.

Burnog M., Kučera A., Cihlářová H., Juřička D. (2022): Possible causes of forest reclamation decline in limestone quarry Mokrá. In: Hemr O., Sedláčková K., Žižlavská N. (eds): SilvaNet-WoodNet 2022: Proceedings Abstracts of Student Scientific Conference, Brno, Nov 25, 2022: 20–22.

Burnog M., Kučera A., Juřička D., Vlček V. (2023): Can lower microbial decomposition be the reason for the decline of reclamation in limestone quarry? In: Chovancová M. (ed.): Student scientific conference PriF UK 2023: Proceeding of Peer-reviewed Papers, Bratislava, Apr 26, 2023: 1051–1056.

Carabassa V., Montero P., Crespo M., Padró J.C., Pons X., Balagué J., Brotons L., Alcañiz J.M. (2020): Unmanned aerial system protocol for quarry restoration and mineral extraction monitoring. Journal of Environmental Management, 270: 1–11.

Chen K., He X., Liang F., Sheng D. (2023): Contribution of capillary pressure to effective stress for unsaturated soils: Role of wet area fraction and water retention curve. Computers and Geotechnics, 154: 1–16.

Cihlářová H. (2017): Effect of soil properties on vegetation types genesis of spontaneously regenerated and forestry reclaimed areas in limestone quarry Mokrá. [Ph.D. Thesis.] Brno, Mendel University in Brno. (in Czech)

Cihlářová H., Koutecký T., Hladký J., Rosická Z., Botková K., Brtnický M., Kynický J. (2017): Can soil properties determine vegetation of spontaneously recovered postmined areas? Case study of limestone quarry Mokrá. Environmental Engineering Science, 34: 638–647.

Cui S., Hough R., Yates K., Osprey M., Kerr C., Cooper P., Coull M., Zhang Z. (2019): Effects of season and sediment-water exchange processes on the partitioning of pesticides in the catchment environment: Implications for pesticides monitoring. Science of the Total Environment, 698: 1–8.

DIN 19539 (2016): Untersuchung von Feststoffen – Temperaturabhängige Differenzierung des Gesamtkohlenstoffs (TOC400, ROC, TIC900). Berlin, Beuth: 20. (in German)

Ferrante D., Oliva G.E., Fernández R.J. (2014): Soil water dynamics, root systems, and plant responses in a semiarid grassland of Southern Patagonia. Journal of Arid Environments, 104: 52–58.

Fu Y., Lu S., Ren T., Horton R., Heitman J.L. (2021): Estimating soil water retention curves from soil thermal conductivity measurements. Journal of Hydrology, 603: 1–8.

Ganapathi H., Phukan M. (2020): Environmental hazards of limestone mining and adaptive practices for environment management plan. In: Singh R.M., Shukla P., Singh P. (eds): Environmental Processes and Management: Tools and Practices. Water Science and Technology Library, Vol. 91. Cham, Springer: 121–134.

Garcia L.G., Salemi L.F., Lima W.P., Ferraz S.F.B. (2018): Hydrological effects of forest plantation clear-cut on water availability: Consequences for downstream water users. Journal of Hydrology: Regional Studies, 19: 17–24.

Hendrychová M., Svobodová K., Kabrna M. (2020): Mine reclamation planning and management: Integrating natural habitats into post-mining land use. Resources Policy, 69: 1–13.

Hillel D. (2004): Introduction to Environmental Soil Physics. Boston, Elsevier Academic Press: 494.

IUSS Working Group WRB (2022): World Reference Base for Soil Resources: International Soil Classification System for Naming Soils and Creating Legends for Soil Maps. 4th Ed. Vienna, International Union of Soil Sciences (IUSS): 236.

Javanshir S., Bayat H., Gregory A.S. (2020): Effect of free swelling index on improving estimation of the soil moisture retention curve by different methods. CATENA, 189: 1–11.

Kaplan Z., Danihelka J., Chrtek J., Kirschner J., Kubát K. Štech M., Štěpánek J. (2019): Klíč ke květeně České republiky. Prague, Academia: 1168. (in Czech)

Leenaars J.G.B., Claessens L., Heuvelink G.B.M., Hengl T., Ruiperez Gonzáles M., van Bussel L.G.J., Guilpart N., Yang H., Cassman K.G. (2018): Mapping rootable depth and root zone plant-available water holding capacity of the soil of sub-Saharan Africa. Geoderma, 324: 18–36.

Lin Z., Qian J., Shi Z. (2022): Estimation of the unsaturated shear strength of expansive soils in relation to capillary water-retention curve. Computers and Geotechnics, 146: 1–8.

Liu J., Chen Z., Kanungo D.P., Song Z., Bai Y., Wang Y., Li D., Qian W. (2019): Topsoil reinforcement of sand slope for preventing erosion using water-based polyurethane soil stabilizer. Engineering Geology, 252: 125–135.

Luna L., Pastorelli R., Bastida F., Hernández T., García C. Miralles I., Solé-Benet A. (2016): The combination of quarry restoration strategies in semiarid climate induces different responses in biochemical and microbiological soil properties. Applied Soil Ecology, 107: 33–47.

Mackovčin P., Jatiová M., Demek J., Slavík P. et al. (2007): Brněnsko. In: Mackovčin P., Jatiová M., Demek J., Slavík P. (eds): Chráněná území ČR. Vol. IX. Prague, Nature Conservation Agency of the Czech Republic: 277–354. (in Czech)

Nanko K., Ugawa S., Hashimoto S., Imaya A., Kobayashi M., Sakai H., Ishizuka S., Miura S., Tanka N., Takahaski M., Kaneko S. (2014): A pedotransfer function for estimating bulk density of forest soil in Japan affected by volcanic ash. Geoderma, 213: 36–45.

Neri A., Sánchez L.E. (2010): A procedure to evaluate environmental rehabilitation in limestone quarries. Journal of Environmental Management, 91: 2225–2237.

Norouzi S., Sadeghi M., Tuller M., Ebrahimian H., Liaghat A., Jones S.B., de Jonge L.W. (2023): A novel laboratory method for the retrieval of the soil water retention curve from shortwave infrared reflectance. Journal of Hydrology, 626: 1–12.

Ojekanmi A.A., Naeth M.A., Huang S. (2020): Calibration and application of quality-scoring functions using soil-forest productivity relationships in land reclamation. Ecological Indicators, 113: 1–12.

Ortega R., Domene M.A., Soriano M., Sánchez-Marañón M., Asensio C., Miralles I. (2020): Improving the fertility of degraded soils from a limestone quarry with organic

https://doi.org/10.17221/6/2024-JFS

and inorganic amendments to support vegetation restoration with semiarid Mediterranean plants. Soil and Tillage Research, 204: 1–12.

Öztürk H.S., Saygin S.D., Copty N.K., Izci E., Erpul G., Demirel B., Saysel A.K., Babaei M. (2023): Hydro-physical deterioration of a calcareous clay-rich soil by sodic water in Central Anatolia, Türkiye. Geoderma Regional, 33: 1–9.

Pečan U., Pintar M., Mihelič R., Kastelec D. (2023): Variability of *in situ* soil water retention curves under different tillage systems and growing seasons. Soil and Tillage Research, 233: 1–11.

Pham T.A., Hashemi A., Sutman M., Medero G.M. (2023): Effect of temperature on the soil–water retention characteristics in unsaturated soils: Analytical and experimental approaches. Soils and Foundations, 63: 1–21.

Prescott C.E., Frouz J., Grayston S.J., Quideau S.A., Straker J. (2019): Chapter 13 – Rehabilitating forest soils after disturbance. In: Busse M., Giardina C.P., Morris D.M., Page-Dumroese D.S. (eds): Developments in Soil Science. Vol. 36. Amsterdam, Elsevier: 309–343.

Qiu D., Zhu G., Lin X., Jiao Y., Lu S., Liu J., Liu J., Zhang W., Ye L., Li R., Wang Q., Chen L. (2023): Dissipation and movement of soil water in artificial forest in arid oasis areas: Cognition based on stable isotopes. CATENA, 228: 1–12.

Quitt E. (1971): Klimatické oblasti Československa. Prague, Academia: 10. (in Czech)

Scott R.L., Biederman J.A., Hamerlynck E.P., Barron-Gafford G.A. (2015): The carbon balance pivot point of southwestern U.S. semiarid ecosystems: Insights from the 21st century drought. Journal of Geophysical Research: Biogeosciences, 120: 2612–2624.

Sekanina A., Musilová Z. (2011): Projekt posouzení stavu a návrh další péče o rekultivované plochy v lomu Mokrá: Zpráva za rok 2011. Internal materials of the mining company Českomoravský cement a.s. Mokrá, Českomoravský cement a.s.: 121. (in Czech)

Sheoran V., Sheoran A.S., Poonia P. (2010): Soil reclamation of abandoned mine land by revegetation: A review. International Journal of Soil, Sediment and Water, 3: 1–21. Available at: https://scholarworks.umass.edu/intljssw/vol3/iss2/13

Šikula J., Větvička V. (2016): Trávy: Traviny a trávníky v ilustracích Vojtěcha Štolfy a Zdenky Krejčové. Prague, Aventinum: 256. (in Czech)

Soil Survey Staff (2014): Soil Survey Field and Laboratory Methods Manual. Soil Survey Investigations Report No. 51, Version 2.0. Lincoln, U.S. Department of Agriculture, Natural Resources Conservation Service: 487.

Štursa J. (2016): Dřeviny opadavé i stálezelené v ilustracích Věry Ničové. Prague, Aventinum: 511. (in Czech)

Vacek Z., Cukor J., Vacek S., Podrázský V., Linda R., Kovařík J. (2018): Forest biodiversity and production potential of post-mining landscape: Opting for afforestation or leaving it to spontaneous development? Central European Forestry Journal, 64: 116–126.

Vacek Z., Cukor J., Vacek S., Linda R., Prokůpková A., Podrázský V., Gallo J., Vacek O., Šimůnek V., Drabek O., Hájek V., Spasić M., Brichta J. (2021): Production potential, biodiversity and soil properties of forest reclamations: Opportunities or risk of introduced coniferous tree species under climate change? European Journal of Forest Research, 140: 1243–1266.

Vacek Z., Zeidler A., Cukor J., Vacek S., Borůvka V., Šimůnek V., Skoták V., Gallo J. (2023): Sustainable biomass production of introduced spruce species plantations under climate change. Trees, 37: 1781–1799.

Van Genuchten M.T. (1980): A closed-form equation for predicting the hydraulic conductivity of unsaturated soils. Soil Science Society of America Journal, 44: 892–898.

Van Genuchten M.T., Leij F.J., Yates S.R. (1991): The RETC Code for Quantifying the Hydraulic Functions of Unsaturated Soils. Ada, U.S. Environmental Protection Agency: 85.

Walters M.B., Kunkle J.M., Kobe R.K., Farinosi E.J. (2023): Seedling drought responses governed by root traits, site-soil moisture regimes and overstory competition-facilitation. Forest Ecology and Management, 544: 1–13.

Wang Y., Ma R., Zhu G. (2023): Representation of the influence of soil structure on hydraulic conductivity prediction. Journal of Hydrology, 619: 1–12.

Welegedara N.P.Y., Grant R.F., Quideau S.A., Landhäusser S.M., Merlin M., Lloret E. (2020): Modelling plant water relations and net primary productivity as affected by reclamation cover depth in reclaimed forestlands of northern Alberta. Plant and Soil, 446: 627–654.

Zeng Z., Wu W., Li Y., Huang C., Zhang X., Peñuelas J., Zhang Y., Li Y., Huang H., Ren X., Ge Q. (2023): Increasing meteorological drought under climate change reduces terrestrial ecosystem productivity and carbon storage. One Earth, 6: 1326–1339.

Zimák J., Štelcl J., Všianský D. (2018): Reflectance colourimetry as a method for estimating the approximate quantity of non-carbonate components in limestones: A case study in the Mokrá Quarry (Czech Republic). CATENA, 169: 90–95.

Received: January 18, 2024
Accepted: May 15, 2024
Published online: August 13, 2024